This is the accepted version of an article published in IEEE Transactions on Sustainable Energy
https://doi.org/10.1109/TSTE.2022.3156069

Stochastic Optimization of Microgrid Operation With Renewable Generation and Energy Storages

Per Aaslid, *Member, IEEE,* Magnus Korpås, *Member, IEEE,* Michael M Belsnes, *Member, IEEE,* and Olav B Fosso, *Senior Member, IEEE*

***Abstract*—The operation of energy storage systems (ESSs) in power systems where variable renewable energy sources (VRESs) and ESSs must contribute to securing the supply, can be considered as an arbitrage against scarcity. The value of using stored energy instantly must be balanced against its potential future value and future risk of scarcity. This paper proposes a multi-stage stochastic programming model for the operation of microgrids with VRESs, ESSs and thermal generators that is divided into a short- and a long-term model. The short-term model utilizes information from forecasts updated every six hours, while the long-term model considers the value of stored energy beyond the forecast horizon. The model is solved using stochastic dual dynamic programming and Markov chains, and the results show that the significance of accounting for short- and long-term uncertainty increases for systems with a high degree of variable renewable generation and ESSs and limited dispatchable generation capacity.**

***Index Terms*—Energy Management, Variable Renewable Energy Sources, Energy Storage Systems, Stochastic Dual Dynamic Programming, Markov Chains, Quantile Regression**

NOMENCLATURE

Sets and indices

i, j	Markov node indices
i^+	Children of Markov node i
$\omega_i \in \Omega_i$	Set of scenarios at Markov node i
$k \in K$	SDDP iteration index
$n \in \{1, \dots, N\}$	Scenario node sequence number
R	Markov chain root node
$g \in \mathcal{G}$	Set of dispatchable generators
$r \in \mathcal{R}$	Set of renewable generators
$d \in \mathcal{D}$	Set of loads
$e \in \mathcal{E}$	Set of EES
$m \in \mathcal{M}$	Set of markets
$t \in \mathcal{T}_i$	Set of timesteps in node i
$\underline{t}_i, \bar{t}_i$	First and last time step in $\mathcal{T}_i$

Parameters

ϕ_{ij}	Transition probability from Markov node i to j
ΔT_i	Time step length at time t
CG_g	Generation cost of generator g
CP_m/CS_m	Purchase/sale price in market m
CD_d	Load shedding cost of demand d
CE_e	Fixed SMV of EES e
PG_g^{max}	Maximum power generation generator g
$PR_{r,i}^{max}$	Renewable generator r power forecast at time t
PM_m^p/PM_m^s	Maximum purchase/sale power at market m
$PD_{d,i}$	Active power demand (before load shedding) by load d at time t
$PS_{e,t}^c/PS_{e,t}^d$	Maximum charge/discharge power of EES e at time t
SOC_e^{min}/SOC_e^{max}	Minimum/maximum SOC of EES e
η_e^c/η_e^d	Charge/discharge efficiency of EES e

Variables and functions

x_i/x_i'	Incoming/outgoing state variables at Markov node i
$\bar{x}_i$	Incoming state dummy variable at Markov node i
u_i	Control variable at Markov node i
ω_i	Random variable at Markov node i
λ_i	State dual variable of solution at Markov node i
θ_i	SDDP cut variable at Markov node i
α_i^k, β_i^k	SDDP cut coefficients at Markov node i, iteration k
$U_i(x_i, \omega_i)$	Control variable feasibility set at Markov node i
$T_i(x_i, u_i, \omega_i)$	Stage-transition function at Markov node i
$C_i(x_i, u_i, \omega_i)$	Stage-objective function at Markov node i
$V_i(x_i, \omega_i)$	Value function at node i
$SEV_i(x_i)$	Storage end value at node i for state x_i
$SMV_i(x_i)$	Storage marginal value at node i for state x_i
$p_{g,t}$	Power from dispatchable generator g at time t
$p_{r,t}$	Power from renewable generator r at time t
$p_{m,t}^p/p_{m,t}^s$	Power purchase/sale from/to market m at time t
$p_{d,t}$	Power withdrawn by load d at time t
$pls_{d,t}$	Load shedding by load d at time t
$ps_{e,t}^c/ps_{e,t}^d$	Active power charge/discharge to/from EES e at time t
$ps_{e,t}$	Net active power charge to EES e at time t
$soc_{e,t}$	State-of-charge of storage e at time t

P. Aaslid is a PhD student at the Norwegian University of Science and Technology and SINTEF Energy Research. M. M. Belsnes is with SINTEF Energy Research. M. Korpås and O. B. Fosso are with Norwegian University of Science and Technology.

I. INTRODUCTION

VARIABLE renewable energy sources (VRESs), primarily solar photovoltaic (PV) and wind, are expected to be the main electricity sources in the future. The levelized cost of energy (LCOE) of solar PV and onshore wind has been reduced by 77% and 30% respectively in less than ten years [1],

This is the accepted version of an article published in IEEE Transactions on Sustainable Energy
https://doi.org/10.1109/TSTE.2022.3156069

and VRESs stand out as a clean and competitive alternative in the electricity market [2]. Despite their relatively low LCOE, large-scale integration of VRESs impose new challenges in balancing the supply and demand. Energy storage system (ESS) technologies have taken large steps both in terms of technological improvements and cost reduction, and ESSs will probably play an important role in balancing the electricity system.

Traditionally, the electricity system have been organized hierarchically with a relatively small number of centralized dispatchable generators operating to meet an almost inflexible demand. In contrast, VRESs are to great extent distributed, weather-driven and uncertain. Moreover, the market price in today's system is often set for large geographical areas and does not capture the challenges related to distributed generation [3]. With the increasing share of distributed energy resources (DERs), a viable option is to move towards decentralized control [4] to manage the system complexity. Microgrids (MGs) offer a possible way of integrating distributed VRESs and ESSs into the power system [5]–[7]. MGs are capable of operating disconnected from the main grid for a limited time or permanently [8], and remote areas may also be organized as MGs to avoid expensive grid expansions.

In energy-constrained systems, where the capacity of VRESs is high and ESSs replace some of the dispatchable capacity, the ESSs must contribute to secure the supply in periods with low generation from VRESs. The operation of these systems can be considered as balancing dispatchable generation costs against the risk of scarcity [9]. The system's ESSs must be operated to have sufficient high state-of-charge (SOC) for periods with high demand, and they should also have sufficient low SOC upfront periods with high generation from VRESs to minimize generation curtailment. These decisions must account for both the daily variations and uncertainty in demand and solar PV generation, as well as the variations and uncertainty in wind power generation over several days.

Power and energy limitations as well as efficiencies also vary for different ESS technologies. Lithium-ion batteries can deliver and absorb high power with low losses, but for a limited time due to energy limitations. A key factor for large scale integration of VRESs is long-duration energy storage with sufficient low storage capacity cost, and hydrogen stands out as one of the most viable options [10]. For hydrogen ESSs (electrolyzer and fuel cell), the size of the hydrogen tank can be scaled up at modest cost, while the electrolyzer and the fuel cell are expensive to scale up and have poor round-trip efficiency compared to lithium-ion batteries [11]. The combination of power and energy limitations, efficiency losses, and uncertain generation and demand makes the operation optimization problem highly complex, and the long-duration storage necessitates scheduling several days ahead.

Rule-based energy management has been successfully applied for managing DERs, both for experimental systems [12]–[14] and virtual systems [15], [16]. These rule-based methods charge/discharge the respective ESSs based on fixed SOC thresholds and predefined priorities, and their computational performance makes them well suited for integration in a real-time environment. However, they do not utilize knowledge about expected future generation and demand from forecasts.

Information from forecasts can improve the operation strategy by formulating dynamic optimization problems with either deterministic or stochastic generation and load forecasts. The resulting power dispatch or SOC can be used as a reference to a real-time control system where the system is re-optimized using rolling horizon each time where either the forecast or observed state are updated [17]–[19].

Stochastic dynamic programming (SDP) approaches [20] also account for how the uncertainty is revealed stage-wise, and the operation strategy can be adjusted stage-wise as more uncertainty is revealed. Instead of providing an optimal control, it provides an optimal policy which is a set of decision rules on how to respond to a given state at a given time. The storage marginal value (SMV) obtained from the SDP solution also has a useful interpretation with respect to deciding when to use the different ESSs compared to generators using constant marginal cost principles [21]. However, SDP approaches require stage-wise independent noise and the auto-correlation of the scenarios are lost. Uncertainty from VRESs is naturally auto-correlated [22]. Therefore, forecast errors tends to sustain and must be accounted for to prevent the security of supply from worsening.

The operation of ESSs is in reality an infinite horizon optimization problem, and this is particularly important when studying systems where ESSs must be used to prevent extreme prices from, for example, periods of scarcity. A common approach to prevent emptying the ESSs at the end of the optimization period, is to apply a bound on the end SOC, typically for daily planning [23]–[25]. However, this approach is unnecessarily inflexible and prevents utilization of the flexibility beyond the optimization horizon [26]. Solar PV and wind power both have distinct seasonal variation, hence the operation method should also be verified through a whole year as in [15], [16], but these only consider rule-based approaches.

Existing literature often studies ESSs' capabilities to minimize thermal power generation and reduce CO_2 emissions, but very few papers consider how ESSs should be operated if they must contribute to prevent extreme prices and scarcity. The valuation of stored energy beyond the optimization period has therefore gained little attention. However, research on large-scale hydropower has paid more attention to infinite horizon optimization both with SDP [27] and stochastic dual dynamic programming (SDDP) [28].

This paper presents a multi-stage stochastic programming (MSSP) energy management model that is solved using a combination of SDP and SDDP [28], [29]. Unlike most previous studies, we address energy-constrained systems where the ESSs are decisive to prevent scarcity. While previous approaches consider forecast uncertainty [17], [19], our model also accounts for the uncertainty beyond the forecast horizon with a separate stochastic long-term model. Moreover, we do not enforce rigorous state end value constraints [23]–[25], but approximate state and time dependent storage end value functions. The storage end value functions are updated monthly to account for seasonal variations and represents infinite horizon similar to approaches applied for hydropower

This is the accepted version of an article published in IEEE Transactions on Sustainable Energy
https://doi.org/10.1109/TSTE.2022.3156069

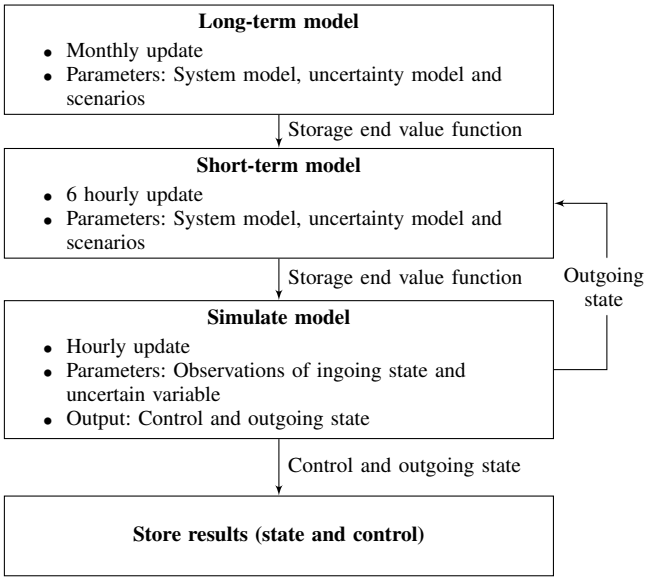

Fig. 1. Summary of stochastic optimization method

scheduling [27]. To overcome the limitations of using stage-wise independent noise, we address the auto-correlation in wind uncertainty to maintain adequate security of supply.

Moreover, we bridge the gap between rule-based [12]–[16] and optimization-based [17]–[19] operation by showing how the solution of the stage-wise optimization problems can be translated into a set of time and state dependent rules, and investigate how these adaptive rules perform compared to static rules for the operation of an actual MG over almost a full year. Stochastic scenarios are generated using gradient boosting quantile regression.

The remainder of this paper is organized as follows: Section II describes the method, section III presents and discusses the results from the application of the method, while section IV provides the conclusions.

II. Method

The proposed method divides the decision process into multiple stages where the stages within the look-ahead of the forecasts are categorized as the short-term model and the stages beyond the forecast horizon as the long-term model. The short-term model stage length follow the frequency of the weather forecast updates, while the long-term model stage length is one day and repeated cyclically.

As illustrated in Fig. 1, the long-term model is solved first. It considers typical seasonal weather, in this case for the present month. Therefore, it is only re-optimized every month as decribed in section II-D. Thereafter, the short-term model is solved using scenarios based on the most recent weather forecast that are updated six-hourly as described in section II-E. Based on the short-term strategy, the optimal control is obtained for the observed state, generation and demand. Finally, the results are saved. The stages and models are connected using the storage end value (SEV) functions as described mathematically in section II-A and interpreted in section II-C.

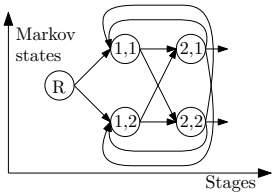

Fig. 2. Example of policy graph as a Markov chain.

A. Stochastic dual dynamic programming

MSSP represents the stage-wise decision process where new uncertainty is revealed and control decisions are taken stage-wise. The solution of an MSSP model is therefore not a sequence of controls, but rather a sequence of decision-rules, often referred to as policies, on how to respond to a given state and for the revealed uncertainty. This is an important difference from the classical two-stage stochastic model [30] where the optimal control is obtained by assuming all uncertainty is revealed at once.

The MSSP model variables are classified into state x_t, control u_t and random variable ω_t where the objective is to find a set of admissible controls (1c) that minimizes the expected stage-wise operating costs for all stages (1a). The state transitions function (1b) describes how the state changes for a given scenario ω_t and control u_t, representing decisions taken both explicitly and implicitly.

$$\min_{u_t}\Bigg\{C_1(x_1,u_1,\omega_1)+\mathop{\mathbb{E}}_{\omega_2|\omega_1}\Bigg[\min_{u_2}\Big(C_2(x_2,u_2,\omega_2)+\ldots + \mathop{\mathbb{E}}_{\omega_T|\omega_{T-1},\ldots,\omega_2}\Big[\min_{u_T}\big(C_T(x_T,u_T,\omega_T)\big)\Big]\Big)\Bigg]\Bigg\} \quad (1a)$$

$$\text{s.t.} \quad x_{t+1}=T_t(x_t,u_t,\omega_t) \quad (1b)$$

$$u_t \in U_t(x_t,\omega_t) \quad (1c)$$

$$\forall t \in \mathcal{T}$$

The MSSP formulation is an optimization problem with nested expected values of optimization problems, and where the random variable at each stage depends on all previous random variables. The size of the extensive problem becomes too large to solve even for problems of modest size. MSSP models are therefore commonly solved with dynamic programming, where the full problem is decomposed into a sequence of stage-wise problems.

This paper considers SDDP [31] for solving the proposed MSSP problem. SDDP requires a convex problem formulation [32] and stage-wise independent random variables. Similar to SDP [33], SDDP divides the full problem into smaller stage-wise problems, and approximates the future cost for each stage using backward recursion. Whereas SDP discretizes the state space, SDDP utilizes the convex problem formulation and approximates the future cost iteratively using multiple linear hyperplanes which serve as lower bounds for the future cost.

A common approach for managing the stage-wise dependent random variables, are to model them as state variables using an auto-regressive model [34]. These can be both additive

This is the accepted version of an article published in IEEE Transactions on Sustainable Energy
https://doi.org/10.1109/TSTE.2022.3156069

and multiplicative [35] depending on the random variable properties, but require a linear model formulation. However, this paper uses a combination of SDDP and SDP with Markov chains [29]. The sequence of stages and the corresponding Markov states can be described with a policy graph [28] as illustrated in Fig. 2: Each node is associated with a stage representing a discrete moment in time, and a Markov state which captures discrete states not included in the state variable x_i. Each node i has a set of children i^+ representing the next stage for the different Markov states. The transition probability between nodes ϕ_{ij} is positive if j is a child of i and otherwise zero.

Given that all future decisions are optimal from a given node and onward, the optimal decision for a previous node can be found with backward recursion using Bellman's principle of optimality [33] by reformulating the model in (1a) to (1c) as shown in (2a) to (2d).

$$V_i(x_i, \omega_i) = \min_{u_i} \Big\{ C_i(x_i, u_i, \omega_i) - SEV_i(x_i') \Big\} \tag{2a}$$

$$SEV_i(x_i') = - \mathop{\mathbb{E}}_{j \in i^+,\ \omega_j \in \Omega_j} \big[V_j\left(x_i', \omega_j\right) \big] \tag{2b}$$

$$\text{s.t.} \quad x_i' = T_i(x_i, u_i, \omega_i) \tag{2c}$$

$$u_i \in U_i(x_i, \omega_i) \tag{2d}$$

The recursive formulation can be solved with SDDP and the algorithm can be divided into two phases: forward and backward pass. In the forward pass, a random sequence of nodes $i^1, \ldots, i^N$ is sampled from the Markov model, and a random scenario $\omega_i \in \Omega_i$ is sampled for each node. The Markov model can also be cyclic to represent infinite horizon where the probability of entering a cycle must be less than one to ensure that the future value produces a finite sum. For the example illustrated in Fig. 2, the outgoing edges from node (2,1) and (2,2) will each sum up to the cycling discount factor [28]. The algorithm also enforces a maximum number of subsequent nodes. For the randomly sampled sequence of nodes and scenarios, the optimization problem (3a) to (3e) is solved sequentially using the outgoing state of previous node as the ingoing state to the next node. When a random scenario has been solved through all stages, the backward pass can start. For each node i and state x_i in the sequence $i^1, \ldots, i^N$, (3a) to (3e) is solved for all outgoing nodes $j \in i^+$ and all scenarios $\omega_j \in \Omega_j$. The resulting objectives $V_j^K(\hat{x}, \omega_j)$ and dual values λ_j are used to calculate a linear hyperplane (3e) for the current node i. The whole procedure is repeated until enough hyperplanes have been added to represent the future cost functions sufficiently accurate. Detailed algorithms are provided in reference [28].

$$V_i^K(\bar{x}_i, \omega_i) = \min_{u_i, x_i, x_i', \theta_i} C_i(x_i, u_i, \omega_i) + \theta_i \tag{3a}$$

$$\text{s.t. } x_i = \bar{x}_i, \quad [\lambda_i] \tag{3b}$$

$$x_i' = T_i(x_i, u_i, \omega_i) \tag{3c}$$

$$u_i \in U_i(x_i, \omega_i) \tag{3d}$$

$$\theta_i \geq \alpha_i^k + \beta_i^k x_i', \quad k \in \{1, 2, \ldots, K\} \tag{3e}$$

Unlike SDP, where the entire state space is explored, SDDP explores the most interesting states based on sampling from the uncertainty distribution.

B. Mathematical description

The detailed mathematical description below is repeated for each node i. Incoming state x_i is the initial SOC $soc_{e,t-1}$ for the first time step in each node, and the outgoing state x_i' is the SOC $soc_{e,t}$ for the final step in each node. The random variable ω_i includes the maximum generation from VRESs (5), such that they can be freely curtailed at no cost, and the demand (6). The admissible controls includes all the remaining constraints.

Dispatchable generators can adjust the generation between zero and maximum generation continuously (4), while the VRES generators have time dependent upper bounds given by weather conditions (5). The demand is also variable in time and load shedding can be applied if the system has insufficient capacity (6). Power can be injected and withdrawn from the ESSs at constant efficiency (7a), but the SOC limits must be respected (7b) and the charge and discharge power must stay within their limits (7c) and (7d). The change in SOC and power limits due to degradation are relatively small for the studied interval and has not been considered. The operation costs due to lifetime reduction for ESSs has neither been considered, but has been addressed for future work. In grid-connected mode, the system can exchange power with an external market within the transmission limits (8a) and (8b). The power injected and withdrawn must be balanced at all time (9). The objective is to minimize the cost of dispatchable generation, net import and load shedding (10).

$$0 \leq p_{g,t} \leq PG_g^{max}, \quad \forall g \in \mathcal{G}, t \in \mathcal{T}_i \tag{4}$$

$$0 \leq p_{r,t} \leq PR_{r,t}^{max}(\omega_t), \quad \forall r \in \mathcal{R}, t \in \mathcal{T}_i \tag{5}$$

$$p_{d,t} = PD_{d,t}(\omega_t) - pls_{d,t} \geq 0, \quad \forall d \in \mathcal{D}, t \in \mathcal{T}_i \tag{6}$$

$$soc_{e,t} = soc_{e,t-1} + \Delta T_t \left(\eta^c ps_{e,t}^c - \frac{ps_{e,t}^d}{\eta^d} \right) \tag{7a}$$

$$SOC_e^{min} \leq soc_{e,t} \leq SOC_e^{max} \tag{7b}$$

$$0 \leq ps_{e,t}^c \leq PS_{e,t}^c \tag{7c}$$

$$0 \leq ps_{e,t}^d \leq PS_{e,t}^d \tag{7d}$$

$$\forall e \in \mathcal{E}, t \in \mathcal{T}_i$$

$$0 \leq p_{m,t}^p \leq PM_m^p \tag{8a}$$

$$0 \leq p_{m,t}^s \leq PM_m^s \tag{8b}$$

$$\forall m \in \mathcal{M}, t \in \mathcal{T}_i$$

$$\sum_{g \in \mathcal{G}} p_{g,t} + \sum_{r \in \mathcal{R}} p_{r,t} + \sum_{m \in \mathcal{M}} p_{m,t}^p + \sum_{e \in \mathcal{E}} ps_{e,t}^d = \sum_{d \in \mathcal{D}} p_{d,t} + \sum_{m \in \mathcal{M}} p_{m,t}^s + \sum_{e \in \mathcal{E}} ps_{e,t}^c, \ t \in \mathcal{T}_i \tag{9}$$

$$\min \sum_{t\in\mathcal{T}_i}\left\{\sum_{g\in\mathcal{G}} CG_g\ p_{g,t} + \sum_{d\in\mathcal{D}} CD_d\ pls_{d,t} + \sum_{m\in\mathcal{M}}\left[CP_m\ p^p_{m,t} - CS_m\ p^s_{m,t}\right]\right\} \quad (10)$$

C. Model interpretation

The optimal energy management of a small-scale power system can be considered as the decision process of meeting the energy demand using the available resources with the lowest marginal operating cost. The marginal cost of dispatchable generators is mainly given by the fuel and emission costs, while VRESs have marginal operating costs close to zero. The value of lost load (VOLL) represents the cost of not being able to meet the demand, and is normally assigned a high value [36]. Since the ESSs neither consume nor deliver energy, but shift energy in time, the marginal cost/value can be considered as the future opportunity cost/value given they are dispatched perfectly in the future. Therefore, they will vary between zero and the VOLL since the energy charged to an ESS can originate from VRESs, and the discharged energy can prevent loss of load [21].

The objective in (2a) has two terms: the stage-objective and the SEV function. The stage-objective is a function of the control variable, while the SEV function is a function of the state. The marginal operating cost of dispatchable generators, demand, purchase and sale are all time and state independent (11), and the optimal dispatch can easily be obtained by picking the unit with the lowest marginal cost first.

$$\begin{aligned}\frac{\partial C_i(x_i,u_i,\omega_i)}{\partial p_{g,t}} &= CG_g, \quad \frac{\partial C_i(x_i,u_i,\omega_i)}{\partial pls_{d,t}} = CD_d \\ \frac{\partial C_i(x_i,u_i,\omega_i)}{\partial p^p_{m,t}} &= CP_m, \quad \frac{\partial C_i(x_i,u_i,\omega_i)}{\partial p^s_{m,t}} = -CS_m\end{aligned} \quad (11)$$

The marginal charge and discharge cost of an ESS is both time and state dependent and can be expressed as a function of the SMV, the marginal value of the SEV function with respect to state (12), as shown in (13) and (14).

$$\frac{\partial SEV_i(x_i)}{\partial x_i} = SMV_i(x_i) \quad (12)$$

$$\frac{\partial SEV_i(x'_i)}{\partial ps^c_{e,t}} = \frac{\partial SEV_i(x'_i)}{\partial x'_i}\frac{\partial x'_i}{\partial ps^c_{e,t}} = SMV_i(x'_i)\cdot\eta^c \quad (13)$$

$$\frac{\partial SEV_i(x'_i)}{\partial ps^d_{e,t}} = \frac{\partial SEV_i(x'_i)}{\partial x'_i}\frac{\partial x'_i}{\partial ps^d_{e,t}} = -SMV_i(x'_i)\cdot\frac{1}{\eta^d} \quad (14)$$

When the SMV function is known, the operation strategy of both generators, loads and ESSs can be translated into a set of time and state dependent decision-rules where the resources with the lowest marginal operating costs are chosen similar to the rule-based approaches in references [12]–[16]. However, the proposed rules based on SMV are both time and state dependent and will therefore consider the future generation and demand under uncertainty.

D. Long-term model

The long-term model uses 24-hour scenarios which are representative for the time of day and year, in this case the respective month, to represent the expectation beyond the forecast horizon. The SDDP algorithm is typically run from a known initial state. In this case, the outgoing state of the short-term model which is the incoming state of the planning is not known ahead, hence the initial Markov state and state variable value are randomized to ensure the model to be sufficiently explored by the algorithm. Since the problem is, in reality, an infinite horizon problem, a cyclic Markov model is used [28]. The cyclic Markov model permits transition from the nodes representing the final stage back to nodes representing previous stages, in this case 24 hours back, with probability 0.8. This will represent an infinite horizon with a discount and prevents the ESSs from emptying after 24 hours. This decomposition permits updating the long-term strategy monthly instead of six-hourly.

1) Wind power: The main purpose of the long-term model is to predict net power balance over several days. Wind power is the dominant energy source and has an evident auto-correlation. The long-term model assumes constant daily wind power generation using five scenarios represented as individual Markov states. The scenarios are generated based on the 24-hourly mean values of historical wind power observations which are sorted and divided into intervals of relative size $0.1, 0.2, 0.4, 0.2, 0.1$. The mean value of each interval represents the scenario. The transition probabilities between the scenarios are obtained using the method described in section II-J.

2) Solar PV power: Clearness index (CI) is a number between zero and one and gives the ratio between solar PV power generation and the clear sky generation at that particular time. The CIs are calculated for the historical observations where hours with zero generation are neglected to avoid zero division. The mean daily CIs are sorted and divided into three equally sized intervals. The mean value for each interval is used as the CI for the long-term model scenarios. The auto-correlation has not been considered to keep the number of Markov states sufficiently low, and since wind is the dominant power source.

3) Demand power: The demand scenarios are generated using quantile regression with the hour of day and the month of year as explanatory variables. The scenarios are given by the $0.1, 0.5, 0.9$ quantiles with probability $0.2, 0.6, 0.2$. The quantile regression method is further described in section II-J.

E. Short-term model

The short-term model stage length is equal to the weather forecast update frequency, six hours, and the forecasts have 60 hours look-ahead yielding ten stages.

1) Wind power: The ratio between wind speed and power generation is non-convex [37] and has increasing variability with increasing wind speed [35]. Wind power scenarios are generated using the $0.1, 0.3, 0.5, 0.7, 0.9$ quantiles, each with 0.2 probability, where each scenario represents a Markov state. The quantile regression model is fitted using the following explanatory variables: wind power forecast at turbine height, wind speed forecast, wind direction forecast, look-ahead hours and last observed power before the forecast period.

This is the accepted version of an article published in IEEE Transactions on Sustainable Energy
https://doi.org/10.1109/TSTE.2022.3156069

The wind speed v_{ref} is forecasted at a reference height h_{ref} which usually differs from the turbine height $h_{turbine}$. Therefore, the turbine wind speed $v_{turbine}$ is scaled using the power law profile [38] shown in (15).

$$v_{turbine} = v_{ref} \left(\frac{h_{turbine}}{h_{ref}} \right)^{k} \tag{15}$$

The roughness factor k is an empirical value for the roughness of the terrain around the wind turbine. Transition probabilities are obtained as described in section II-J.

2) Solar PV power: Solar power explanatory variables are: cloud area fraction forecast, normalized maximum solar power, initial solar power and look-ahead hours. The normalized maximum solar power represents the theoretical maximum generation for that time of day and year as a number between zero and one. There are theoretical methods for determining this value given the geographical location, and the panel direction and tilt. Since panel angle and direction as well as seasonal configurations are unknown for the case in this paper, the normalized maximum solar power has been approximated using historically observed generation by assuming the normalized maximum solar power is given by the maximum observed value at that day and hour plus/minus nine days for all observed years.

3) Demand power: The demand will use the same regression model as the long-term model described in section II-D3.

F. Simulation

To verify the value of the different optimization strategies, historical observations are simulated with rolling horizon. For each observed value, the corresponding node i is identified based on the Markov state and stage, and the optimal control is found by solving (3a) to (3e). The optimal control and the resulting state are saved, and the procedure is repeated for the next stage using the previous outgoing state as the incoming state. The short- and long-term models are updated as shown in Fig. 1.

G. Reference models

1) Perfect foresight: The perfect foresight model uses the mathematical model description from section II-B but optimizes the whole period at once with the actual historical generations and demand instead of using forecasts. The SEV at the end of the optimization is set using the fixed SMV described in section II-G3. The perfect foresight model can be considered as a theoretical absolute lower bound of the operating costs.

2) Deterministic model: The deterministic model formulation uses the same mathematical model description presented in section II-B as the stochastic model, but with least square point forecasts for generation from VRESs and demand instead of multiple scenarios, stages and Markov states. The deterministic model only considers the short-term model horizon and is similar to references [17], [18].

3) Rule-based model: Rule-based models [12]–[14] use a fixed priority for generators and ESSs to decide where to withdraw lacking or inject surplus energy. Given an arbitrary ESS e with charge/discharge efficiency η_e^c/η_e^d and SMV CE_e, then the cost of discharging one unit will be $\frac{CE_e}{\eta_e^d}$, hereby referred as discharge cost. The corresponding value of charging one unit, the charge value, will be $CE_e\eta_e^c$. If the SMV is chosen such that the discharge cost is less than the diesel generation cost, the ESS will be used to meet the demand before the diesel generator. Likewise, diesel will not be used to charge the ESS as long the charge value is less than the diesel cost, and the ESS with highest charge value will be charged first when there are surplus generation from VRESs.

The cases with fixed end value will use SMV 80 €$/MWh$ for both ESSs. Since the charge value is less than the marginal cost of the diesel generator, both of the ESSs will only be charged when there are surplus generation from VRESs. The discharge value of the battery is less than the diesel generator marginal cost or the grid purchase price, hence it will displace diesel generation or import whenever possible. However, the discharge value of hydrogen is higher. Consequently, it will only be used to prevent load shedding.

H. Implementation

The proposed method has been implemented in the programming language Julia (1.4.2) using the toolbox SDDP.jl (0.3.14) [39] and Gurobi (9.1) for solving the stage-wise linear optimization models. The long-term models were trained with 1000 iterations, and the short-term models with 100 iterations. To simulate the proposed case, 1350 short-term models were trained and simulated in 4-5 hours while the training time for 12 months of the long-term model was around 1.5 hours on a laptop with Intel i7-8650U CPU and 16 GB RAM.

I. Case study

Rye microgrid is located in Central Norway near Trondheim and is partly funded by the Horizon 2020 project REMOTE [40]. The MG comprises a farm and a few residential houses, and the electricity is supplied by solar PV panels and a wind turbine [41]. The turbine height and the reference height are 30 and 10 meters respectively, and the terrain roughness factor is set to 0.3 considering the wind turbine is partially surrounded by forest [42]. There is also a lithium-ion battery and a hydrogen storage unit with an electrolyzer and a fuel cell to balance the load and generation. A diesel generator serves as backup when the VRE generation is persistently low. The generation capacities are 86 and 135 kW for solar PV and wind respectively. The import price and diesel generator operating cost are both 100 €/MWh, while the sale price is 50 €/MWh. The VOLL is 5000 €/MWh. The numerical values of the ESSs are presented in Table I. Diesel and wind power generation capacities in this study have been reduced from the original system to increase the probability of scarcity. This choice is made to study the impact of ESS operation strategies in critical periods of the year where ESSs are needed to prevent load shedding. Time series for historical observed generation and

This is the accepted version of an article published in IEEE Transactions on Sustainable Energy
https://doi.org/10.1109/TSTE.2022.3156069

TABLE I
NUMERICAL VALUES FOR MICROGRID ENERGY STORAGE SYSTEMS.

Description	Unit	Lithium-ion	Hydrogen
Charge power	[kW]	500	55
Discharge power	[kW]	500	100
Size	[kWh]	500	3300
Charge efficiency	[%]	96	64
Discharge efficiency	[%]	96	50

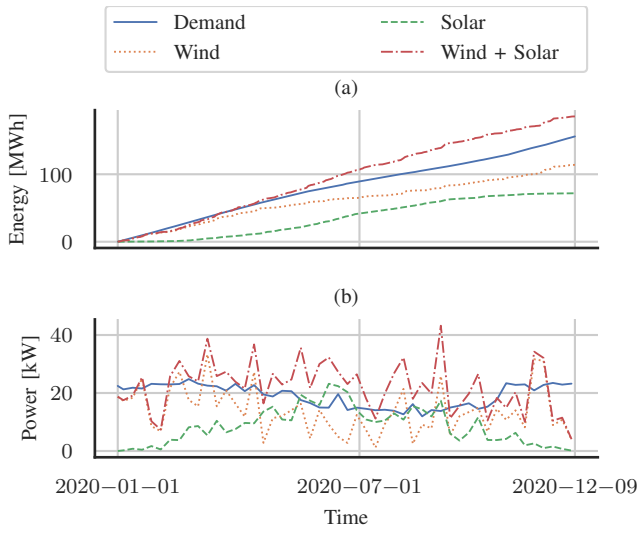

Fig. 3. Accumulated generation and load (a) and weekly average generation and load (b) for the entire studied period.

load, and historical weather forecasts can be downloaded from [43].

The system has sufficient power generation from VRESs in the long run, as shown in Fig. 3a. However, Fig. 3b shows a significant weekly variability, especially for the wind power, that must be balanced with ESSs. For an average daily load above 20 kW, a fully charged lithium-ion battery can meet the load for maximum 24 hours, while a full hydrogen tank can meet the demand for around 80 hours. If the dispatchable generation capacity is low, sufficient stored energy in the ESSs is crucial to prevent load shedding. The analysis period is between 2020-01-01 and 2020-12-09.

J. Quantile regression and transition probability

Generation forecasts for the short-term model are determined based on meteorological weather forecasts from the Norwegian Meteorological Institute with a 60-hour foresight updated every sixth hour. Let $\psi_{t+k|t}$ denote the weather forecast for time $t+k$ issued at time t. The goal is to find a set of scenarios $\Omega_{t+k} = f(\omega_{t-i}, \psi_{t+k|t}, k)$ given previous observations and forecast variables. Unfortunately, it is difficult to include the look-ahead as an explanatory variable in a linear model as the product of two variables is not allowed. Linear models will therefore require a separate regression model for each look-ahead value k [44]. Gradient boosting (GB) is a machine learning technique that can be used for regression by forming an ensemble of weak decision trees [45], [46]. Moreover, GB is not limited to linear combinations, hence the look-ahead can be used directly as an explanatory variable. All training data can therefore be used to fit one model instead of an individual models for each k. This approach will therefore be less dependent on having a large training data set compared to linear regression. The regression has been performed with MLJ.jl (0.16.2) [47] and ScikitLearn (0.24.0) [48] with regularization constant 1.0 and interior-point solver. Deterministic point forecasts are generated using a least square regressor, while scenarios are generated using quantile regression.

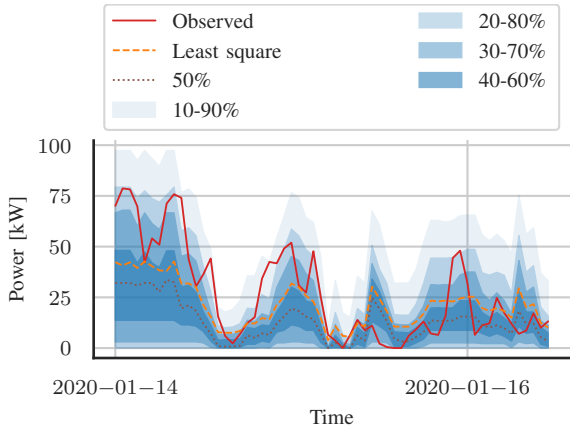

Fig. 4. Example of wind power percentile forecasts (blue) compared to least square forecast and observed power for a 60 hours interval. Percentile median values are used as wind power scenarios for the stochastic optimization. Least square forecast is used for the deterministic optimization.

Let ω_i^α denote the α quantile of a random variable at node i, and $\hat{\omega}_i$ an observed value, then $P(\omega_i^\alpha \geq \hat{\omega}_i) = \alpha$. Moreover, let $\mathbb{E}[\omega_i^\alpha]$ and $\mathbb{E}[\hat{\omega}_i]$ denote the mean value of the respective quantiles and the observed values over time. The observed values at the node i are then in the j'th quantile interval if $\mathbb{E}[\omega_i^{\alpha_{j-1}}] \leq \mathbb{E}[\hat{\omega}_i] < \mathbb{E}[\omega_i^{\alpha_j}]$ where $\alpha = [\alpha_0, \ldots, \alpha_n]$.

The quantile regression model is trained using historical weather forecasts as explanatory variables and the actual generation as the outcome variable. For each historical forecast, the outcome variable is classified into quantile interval and the number of transitions between the quantile intervals is counted. Let the matrix Φ denote the transition counts such that Φ_{ij} denotes the number of transitions between quantile interval i and j, then the resulting transition probability matrix ϕ is given by $\phi_{ij} = \frac{\Phi_{ij}}{\sum_{k=1}^{n} \Phi_{ik}}$. The resulting quantile intervals compared to the point forecast and observed wind power are shown for a random interval in Fig. 4.

III. RESULTS AND DISCUSSION

A. Long-term strategy

As explained in section II-C, generation from VRESs with zero marginal cost is always preferred if available, while the priorities between the dispatchable generation, import, export and ESS charge and discharge varies and are given by the SMV. Fig. 5 illustrates the resulting long-term operation strategy for the ESSs based on the SMVs as a function of both battery SOC (x-axis) and hydrogen SOC (y-axis). The SMV

This is the accepted version of an article published in IEEE Transactions on Sustainable Energy
https://doi.org/10.1109/TSTE.2022.3156069

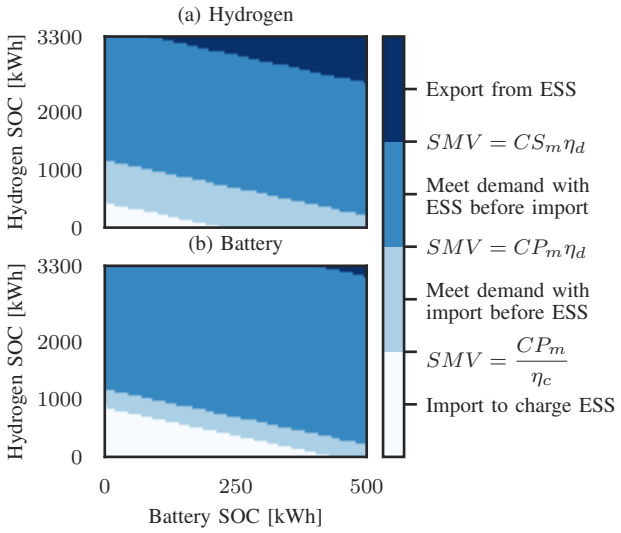

Fig. 5. Long-term model strategy for ESS dispatch based on SMV as a function of battery and hydrogen SOC for the system with $15kW$ import/export capacity in May with intermediate wind speeds (Markov state 3 of 5) for (a) hydrogen and (b) battery. The storage marginal value in the transition between the different areas are shown in the legend and the numerical values are shown in Table I and section II-I.

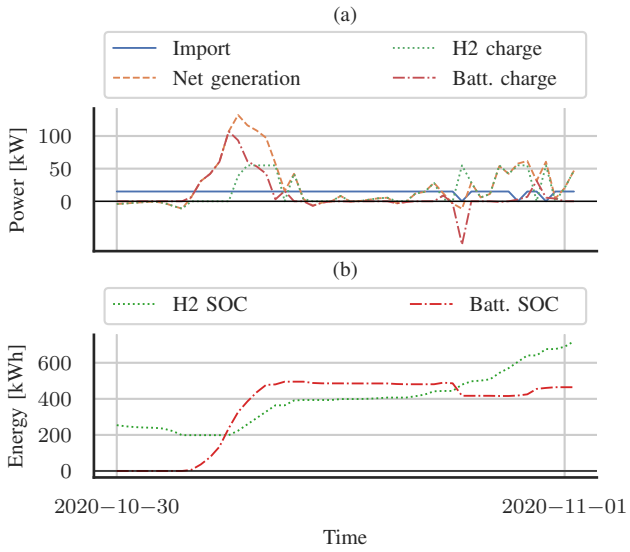

Fig. 6. Snapshot from case 21 where power is imported due to low SOC despite of positive net generation.

boundaries are based on the charge/discharge cost derived in (13) and (14).

Fig. 5 shows that it is optimal to use available import capacity to charge the ESSs when the SOC is sufficiently low. For slightly higher SOC, the optimal strategy is to import instead of using stored energy such that the stored energy is saved for potential future situations with risk of scarcity. When the SOC is sufficiently high, the stored energy should be used to meet the demand instead of import, while when the SOC is close to maximum, the energy should be exported to prevent potential generation curtailment.

A similar strategy can be extracted from the short-term strategy giving even more accurate rules which also considers the short-term generation and load forecasts. Additionally, this makes the proposed method suitable for integration towards real-time systems.

B. Simulation of historical observations

The optimal operation of almost a full year with historical data is summarized in Table II for three conditions of the system: high dispatchable capacity (75 kW), low dispatchable capacity (15 kW) and weakly grid connected system (15 kW import/export capacity). Each condition has been analysed with seven different methods. The first method (cases 1,8 and 15) shows the results with perfect foresight which can be considered as an absolute lower bound of the costs. The remaining methods are different combinations of short- and long-term models, where the stochastic model is our proposed model. The outgoing SOC is shown in Table II, but the value of it is not included in the costs.

The dispatchable generation capacity of $75kW$ of the cases 1-7 is always sufficient to meet the peak demand. Therefore, the load shedding is always zero and the difference in operating cost between the different methods originates from the diesel consumption. The fixed end value (rule-based) of the cases 2-4 is conservative and prioritizes hydrogen for load shedding prevention, which results in a poor utilization of VRE compared to the cut end values from the stochastic long-term model. By also considering the forecast uncertainty in case 4, the utilization of VRESs increase considerably. The stochastic cuts of cases 5-7 adapt the strategy both with respect to SOC, wind state and time of the day and seasonal variations, and position the SOC such that surplus generation can be absorbed efficiently.

Given perfect information (case 8), it is also possible to fully prevent load shedding with a $15kW$ diesel generator through early activation upfront periods with low generation from VRESs to ensure sufficient energy in the system's ESSs. The operating costs are actually slightly less than for case 1 due to lower final hydrogen SOC. The rule-based long-term strategy (cases 9-11), where only surplus generation from VRESs is stored, causes significant load shedding. In contrast, the stochastic long-term model (cases 12-14) almost eliminates load shedding. A key difference is that the stochastic long-term model provides a state dependent valuation of the stored energy, while the rule-based method represents fixed valuation. Therefore, the stochastic long-term model is very thrifty with the stored energy when the SOC is low, which is essential to prevent load shedding. Moreover, the use of weather forecasts (cases 10-11), and in particular with stochastic modeling (cases 13-14), is important to keep both load shedding and diesel generation low. Also note that case 12 has a high utilization of wind and solar compared to 14, but still higher operating costs. The lack of forecast imposes rapid cycling of the hydrogen storage resulting in high efficiency losses, while the stochastic model has less frequent cycling of the hydrogen storage and less losses.

By replacing the diesel generator with a grid connection with equal capacity, the surplus generation can be exported (cases 15-21). The export price is set to half of the import

This is the accepted version of an article published in IEEE Transactions on Sustainable Energy
https://doi.org/10.1109/TSTE.2022.3156069

TABLE II
SUMMARY OF OPERATING COSTS, LOAD SHEDDING, IMPORT, EXPORT, GENERATION AND FINAL EES SOC FOR ALL CASES AND ALL OPTIMIZATION METHODS. NUMBERS IN PARENTHESIS SHOWS PERCENTAGE OF VRES THAT HAS BEEN UTILIZED.

				[€]	Energy $[MWh]$							
	Case	Short-term model	Long-term model	Cost	Load shedding	Diesel	Import	Export	Wind generation	Solar generation	H2 end SOC	Batt. end SOC
Diesel capacity: 75 kW	1	Perfect	-	1957	0.00	19.6	-	-	109.0 (57%)	55.8 (78%)	3.30	0.00
	2	None	Rule-based	2917	0.00	29.2	-	-	83.6 (44%)	50.6 (70%)	3.30	0.00
	3	Deterministic	Rule-based	2988	0.00	29.9	-	-	88.6 (47%)	52.6 (73%)	3.29	0.00
	4	Stochastic	Rule-based	2219	0.00	22.2	-	-	102.4 (54%)	58.6 (82%)	0.58	0.00
	5	None	Stochastic	2341	0.00	23.4	-	-	107.6 (57%)	59.8 (83%)	0.00	0.00
	6	Deterministic	Stochastic	2055	0.00	20.5	-	-	108.3 (57%)	59.3 (83%)	0.00	0.00
	7	Stochastic	Stochastic	1929	0.00	19.3	-	-	105.4 (56%)	56.9 (79%)	0.00	0.00
Diesel capacity: 15 kW	8	Perfect	-	1954	0.00	19.5	-	-	108.9 (57%)	55.6 (77%)	3.15	0.00
	9	None	Rule-based	9267	1.42	21.6	-	-	96.0 (51%)	52.3 (73%)	0.10	0.00
	10	Deterministic	Rule-based	5563	0.61	25.3	-	-	95.6 (50%)	53.5 (74%)	1.33	0.00
	11	Stochastic	Rule-based	3424	0.24	22.2	-	-	104.1 (55%)	58.6 (82%)	0.08	0.00
	12	None	Stochastic	3288	0.00	32.9	-	-	107.6 (57%)	61.5 (86%)	1.73	0.13
	13	Deterministic	Stochastic	2746	0.07	23.9	-	-	106.7 (56%)	55.8 (78%)	1.41	0.00
	14	Stochastic	Stochastic	2354	0.00	23.5	-	-	103.0 (54%)	55.3 (77%)	1.99	0.00
Import/export capacity: 15 kW	15	Perfect	-	632	0.00	-	24.7	36.8	120.2 (63%)	65.2 (91%)	3.15	0.00
	16	None	Rule-based	8610	1.42	-	21.6	13.1	104.3 (55%)	57.1 (79%)	0.10	0.00
	17	Deterministic	Rule-based	4023	0.54	-	26.0	25.2	107.1 (56%)	61.7 (86%)	1.33	0.00
	18	Stochastic	Rule-based	2260	0.27	-	26.5	34.5	117.8 (62%)	64.8 (90%)	0.10	0.00
	19	None	Stochastic	3302	0.11	-	41.9	28.5	115.5 (61%)	64.1 (89%)	1.63	0.13
	20	Deterministic	Stochastic	1918	0.13	-	28.6	32.3	117.5 (62%)	64.8 (90%)	1.13	0.00
	21	Stochastic	Stochastic	1185	0.00	-	28.2	32.9	117.8 (62%)	64.8 (90%)	2.05	0.00

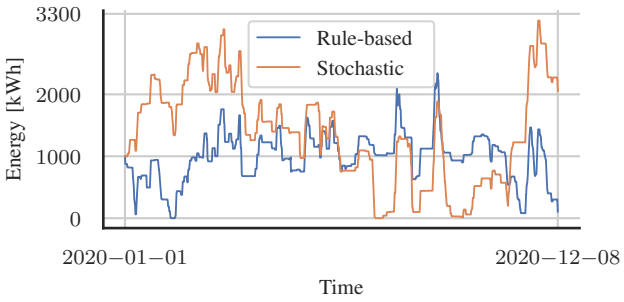

Fig. 7. Comparison of hydrogen SOC for rule-based (case 18) and stochastic long-term model (case 21) with stochastic short-term model through the entire optimization period for the weakly grid connected system.

price, for example due to grid tariffs. The trends are similar to previous cases (8-14), but the differences are even more pronounced. The stochastic short-term models (cases 18 and 21) have both the lowest load shedding and the highest export compared to the equivalent deterministic and no-forecast short-term models. Cases 19 and 21 also have higher outgoing SOC than the corresponding fixed end value cases (16 and 18) making them better prepared to prevent future scarcity.

The snapshot from case 21 in Fig. 6 shows positive import although the net generation (generation from VRESs minus demand) is positive. If the SOC is sufficiently low, it is important to increase the SOC to prevent potential future load shedding. This is also reflected by the brightest area in the long-term strategy shown in Fig. 5.

Fig. 7 shows how the stochastic long-term strategy adapts to seasonal variations compared to the rule-based method. The risk of scarcity is higher through the winter due to higher load and increased probability of sustained low generation from wind compared to solar power. Therefore, the SOC is higher in the beginning and the end of the year for the stochastic long-term model compared to the rule-based long-term model. The stochastic long-term model also permits lower SOC through the summer to enable buffering surplus generation.

Although the results originate from a small-scale power system, they are also relevant to large-scale power systems. To reach net zero emissions towards 2050, 63% of the energy will originate from VRESs with 74% of the total generation capacity [49]. The high share of variable and uncertain generation makes prevention of scarcity and extreme prices increasingly important. The stored hydro-dominated Nordic power system which has been operated as a competitive market where the price has been influenced by the risk of scarcity since the early 1990s [50] shows that this is a feasible direction.

IV. CONCLUSIONS

The work presented in this paper shows the importance of accounting for uncertainty in power systems when more of the dispatchable generation capacity in autonomous systems is replaced by VRESs and ESSs. The proposed multi-stage stochastic programming model has demonstrated a reduction in the operational costs associated with import, export and thermal generation while at the same time increasing the security of supply for the presented isolated microgrid compared to a deterministic point-forecast model and a no-forecast model. The results show a 70% cost reduction when using the stochastic model compared to a deterministic point-forecast model with fixed storage end value for the weakly grid connected system, where 95% of the improvement originates from reduction in load shedding. The model is also able to export excess energy while keeping the risk of load shedding low.

The benefits of the proposed model were most significant for weakly connected systems and systems with low dispatchable generation capacity.

Managing generation and load uncertainty is particularly important in MGs where stored energy is the limiting factor rather than installed capacity. Realistic and robust scheduling models are a key component in the efficient and secure operation of systems with a high share of VRESs and ESSs.

A. Future work

Possible steps towards a more applicable model could be to add more details such as: generation cost curves and efficiency as a function of charge/discharge for ESSs, ESS degradation costs, start/stop costs for generators and ESSs, as well as power flow equations. The proposed improvements will impose new challenges with respect to convexity which can be handled both with convex relaxations and integer variables, and by using stochastic dual dynamic integer programming as solution method [51].

Although SDDP is capable of handling several hundred state variables [52], the use of discrete Markov states to represent uncertainty has clear limitations with respect to dimensionality. Moreover, adding new types of random variables, such as new generation or demand, increases the number of scenarios rapidly. Therefore, random variables must be chosen carefully and can be managed with principal component analysis to reduce the dimensionality, and by using a linear model formulation of the random variables to enable the method to also scale up for larger systems.

ACKNOWLEDGMENT

This work has been funded by the Norwegian Research Council under grant number 272398. The authors would like to thank TrønderEnergi Kraft AS for sharing data from Rye Microgrid.

REFERENCES

[1] International Renewable Energy Agency, *Global energy transformation: A roadmap to 2050 (2019 edition)*, Abu Dhabi, 2019. ISBN 978-92-9260-121-8

[2] C. Kost, S. Shammugam, V. Jülch, H.-T. Nguyen, and T. Schlegl, "Levelized cost of electricity renewable energy technologies," 2018. [Online]. Available: https://www.ise.fraunhofer.de/content/dam/ise/en/documents/publications/studies/EN2018_Fraunhofer-ISE_LCOE_Renewable_Energy_Technologies.pdf (Accessed 2020-09-03).

[3] E. Mengelkamp, J. Gärttner, K. Rock, S. Kessler, L. Orsini, and C. Weinhardt, "Designing microgrid energy markets: A case study: The Brooklyn Microgrid," *Applied Energy*, vol. 210, pp. 870–880, 1 2018.

[4] W. Tushar, C. Yuen, T. K. Saha, T. Morstyn, A. C. Chapman, M. J. E. Alam, S. Hanif, and H. V. Poor, "Peer-to-peer energy systems for connected communities: A review of recent advances and emerging challenges," *Applied Energy*, vol. 282, p. 116131, 1 2021.

[5] M. Yan, M. Shahidehpour, A. Paaso, L. Zhang, A. Alabdulwahab, and A. Abusorrah, "Distribution Network-Constrained Optimization of Peer-to-Peer Transactive Energy Trading among Multi-Microgrids," *IEEE Transactions on Smart Grid*, vol. 12, no. 2, pp. 1033–1047, 3 2021.

[6] H. Karimi and S. Jadid, "Optimal energy management for multi-microgrid considering demand response programs: A stochastic multi-objective framework," *Energy*, vol. 195, p. 116992, 3 2020.

[7] A. Hasankhani and S. M. Hakimi, "Stochastic energy management of smart microgrid with intermittent renewable energy resources in electricity market," *Energy*, vol. 219, p. 119668, 3 2021.

[8] N. Hatziargyriou, H. Asano, R. Iravani, and C. Marnay, "Microgrids," *IEEE Power and Energy Magazine*, vol. 5, no. 4, pp. 78–94, 7 2007.

[9] J. Geske and R. Green, "Optimal Storage, Investment and Management under Uncertainty: It is Costly to Avoid Outages!" *The Energy Journal*, vol. 41, no. 2, 4 2020.

[10] N. A. Sepulveda, J. D. Jenkins, A. Edington, D. S. Mallapragada, and R. K. Lester, "The design space for long-duration energy storage in decarbonized power systems," *Nature Energy 2021 6:5*, vol. 6, no. 5, pp. 506–516, 3 2021.

[11] M. A. Pellow, C. J. Emmott, C. J. Barnhart, and S. M. Benson, "Hydrogen or batteries for grid storage? A net energy analysis," *Energy and Environmental Science*, vol. 8, no. 7, pp. 1938–1952, 7 2015.

[12] L. Valverde, F. Rosa, and C. Bordons, "Design, planning and management of a hydrogen-based microgrid," *IEEE Transactions on Industrial Informatics*, vol. 9, no. 3, pp. 1398–1404, 2013.

[13] Y. Han, G. Zhang, Q. Li, Z. You, W. Chen, and H. Liu, "Hierarchical energy management for PV/hydrogen/battery island DC microgrid," *International Journal of Hydrogen Energy*, vol. 44, no. 11, pp. 5507–5516, 2 2019.

[14] H. Yang, Q. Li, S. Zhao, W. Chen, and H. Liu, "A Hierarchical Self-Regulation Control for Economic Operation of AC/DC Hybrid Microgrid with Hydrogen Energy Storage System," *IEEE Access*, vol. 7, pp. 89 330–89 341, 2019.

[15] A. Kafetzis, C. Ziogou, K. D. Panopoulos, S. Papadopoulou, P. Seferlis, and S. Voutetakis, "Energy management strategies based on hybrid automata for islanded microgrids with renewable sources, batteries and hydrogen," *Renewable and Sustainable Energy Reviews*, vol. 134, p. 110118, 12 2020.

[16] A. Monforti Ferrario, F. Vivas, F. Segura Manzano, J. Andújar, E. Bocci, and L. Martirano, "Hydrogen vs. Battery in the Long-term Operation. A Comparative Between Energy Management Strategies for Hybrid Renewable Microgrids," *Electronics*, vol. 9, no. 4, p. 698, 4 2020.

[17] R. Palma-Behnke, C. Benavides, F. Lanas, B. Severino, L. Reyes, J. Llanos, and D. Saez, "A microgrid energy management system based on the rolling horizon strategy," *IEEE Transactions on Smart Grid*, vol. 4, no. 2, pp. 996–1006, 2013.

[18] M. Elkazaz, M. Sumner, and D. Thomas, "Energy management system for hybrid PV-wind-battery microgrid using convex programming, model predictive and rolling horizon predictive control with experimental validation," *International Journal of Electrical Power and Energy Systems*, vol. 115, p. 105483, 2 2020.

[19] M. Petrollese, L. Valverde, D. Cocco, G. Cau, and J. Guerra, "Real-time integration of optimal generation scheduling with MPC for the energy management of a renewable hydrogen-based microgrid," *Applied Energy*, vol. 166, pp. 96–106, 3 2016.

[20] A. G. Bakirtzis and E. S. Gavanidou, "Optimum operation of a small autonomous system with unconventional energy sources," *Electric Power Systems Research*, vol. 23, no. 2, pp. 93–102, 3 1992.

[21] P. Aaslid, M. Korpås, M. M. Belsnes, and O. B. Fosso, "Pricing electricity in constrained networks dominated by stochastic renewable generation and electric energy storage," *Electric Power Systems Research*, vol. 197, p. 107169, 8 2021.

[22] A. Michiorri, J. Lugaro, N. Siebert, R. Girard, and G. Kariniotakis, "Storage sizing for grid connected hybrid wind and storage power plants taking into account forecast errors autocorrelation," *Renewable Energy*, vol. 117, pp. 380–392, 3 2018.

[23] H. Shuai, J. Fang, X. Ai, Y. Tang, J. Wen, and H. He, "Stochastic optimization of economic dispatch for microgrid based on approximate dynamic programming," *IEEE Transactions on Smart Grid*, vol. 10, no. 3, pp. 2440–2452, 5 2019.

[24] M. Sedighizadeh, M. Esmaili, A. Jamshidi, and M. H. Ghaderi, "Stochastic multi-objective economic-environmental energy and reserve scheduling of microgrids considering battery energy storage system," *International Journal of Electrical Power and Energy Systems*, vol. 106, pp. 1–16, 3 2019.

[25] H. Moradi, M. Esfahanian, A. Abtahi, and A. Zilouchian, "Optimization and energy management of a standalone hybrid microgrid in the presence of battery storage system," *Energy*, vol. 147, pp. 226–238, 3 2018.

[26] I. Sperstad and M. Korpås, "Energy Storage Scheduling in Distribution Systems Considering Wind and Photovoltaic Generation Uncertainties," *Energies*, vol. 12, no. 7, p. 1231, 3 2019.

[27] O. Wolfgang, A. Haugstad, B. Mo, A. Gjelsvik, I. Wangensteen, and G. Doorman, "Hydro reservoir handling in Norway before and after deregulation," *Energy*, vol. 34, no. 10, pp. 1642–1651, 10 2009.

[28] O. Dowson, "The policy graph decomposition of multistage stochastic optimization problems," *Networks*, vol. 76, no. 1, pp. 3–23, 2020.

[29] A. Gjelsvik, M. M. Belsnes, and A. Haugstad, "An algorithm for stochastic medium-term hydrothermal scheduling under spot price uncertainty," in *Proc. 13th Power System Computation Conference*, Trondheim, Norway, 1999, pp. 1079–1085.
[30] J. R. Birge and F. Louveaux, *Introduction to Stochastic Programming*, 2nd ed., ser. Springer Series in Operations Research and Financial Engineering. New York, NY: Springer New York, 2011. ISBN 978-1-4614-0236-7
[31] M. V. F. Pereira and L. M. V. G. Pinto, "Multi-stage stochastic optimization applied to energy planning," *Mathematical Programming*, vol. 52, no. 1-3, pp. 359–375, 5 1991.
[32] P. Girardeau, V. Leclere, and A. B. Philpott, "On the convergence of decomposition methods for multistage stochastic convex programs," *Mathematics of Operations Research*, vol. 40, no. 1, pp. 130–145, 2 2015.
[33] R. E. Bellman, *Dynamic Programming*. Dover Publications, 2003. ISBN 9780486428093
[34] A. Shapiro, "Analysis of stochastic dual dynamic programming method," *European Journal of Operational Research*, 2011.
[35] A. Papavasiliou, Y. Mou, L. Cambier, and D. Scieur, "Application of Stochastic Dual Dynamic Programming to the Real-Time Dispatch of Storage under Renewable Supply Uncertainty," *IEEE Transactions on Sustainable Energy*, vol. 9, no. 2, pp. 547–558, 4 2018.
[36] S. Stoft, *Power System Economics: Designing Markets for Electricity*. IEEE Press, 2002. ISBN 9780470545584
[37] "Vestas V27." [Online]. Available: https://en.wind-turbine-models.com/turbines/9-vestas-v27 (Accessed 2021-06-18).
[38] J. F. Manwell, J. G. McGowan, and A. L. Rogers, *Wind energy explained: theory, design and application.* John Wiley & Sons, 2010. ISBN 978-0-470-01500-1
[39] O. Dowson and L. Kapelevich, "SDDP.jl: A julia package for stochastic dual dynamic programming," *INFORMS Journal on Computing*, vol. 33, no. 1, pp. 27–33, 12 2021.
[40] "Remote EU project," 2021. [Online]. Available: https://www.remote-euproject.eu/remote-project/ (Accessed 2021-06-17).
[41] P. Marocco, D. Ferrero, M. Gandiglio, and M. Santarelli, "Remote area Energy supply with Multiple Options for integrated hydrogen-based TEchnologies - Deliverable number 2.2," 2018. [Online]. Available: https://www.remote-euproject.eu/remote18/rem18-cont/uploads/2019/03/REMOTE-D2.2.pdf (Accessed 2021-06-17).
[42] World Meteorological Organization, "Guide to Meteorological Instruments and Methods of Observation," 2008. [Online]. Available: https://www.weather.gov/media/epz/mesonet/CWOP-WMO8.pdf (Accessed 2021-04-12).
[43] P. Aaslid, "Rye microgrid load and generation data, and meteorological forecasts." 2021. [Online]. Available: https://doi.org/10.5281/zenodo.4448894 (Accessed 2021-06-21).
[44] P. Pinson, H. Madsen, H. A. Nielsen, G. Papaefthymiou, and B. Klöckl, "From probabilistic forecasts to statistical scenarios of short-term wind power production," *Wind Energy*, vol. 12, no. 1, pp. 51–62, 1 2009.
[45] G. Ridgeway, "Generalized Boosted Models: A guide to the gbm package," 2020. [Online]. Available: https://cran.r-project.org/web/packages/gbm/vignettes/gbm.pdf (Accessed 2021-06-17).
[46] J. H. Friedman, "Greedy Function Approximation: A Gradient Boosting Machine," *The Annals of Statistics*, vol. 29, no. 5, pp. 1189–1232, 6 2001.
[47] A. D. Blaom, F. Kiraly, Y. Simillides, D. Arenas, T. Lienart, and S. J. Vollmer, "MLJ: A Julia package for composable machine learning," *The Journal of Open Source Software*, vol. 5, no. 55, p. 2704, 7 2020.
[48] F. Pedregosa, G. Varoquaux, A. Gramfort, V. Michel, B. Thirion, O. Grisel, M. Blondel, P. Prettenhofer, R. Weiss, V. Dubourg, J. Vanderplas, A. Passos, D. Cournapeau, M. Brucher, M. Perrot, and E. Duchesnay, "Scikit-learn: Machine Learning in Python," *Journal of Machine Learning Research*, vol. 12, pp. 2825–2830, 2011.
[49] International Renewable Energy Agency, *WORLD ENERGY TRANSITIONS OUTLOOK 1.5° C PATHWAY*, 2021. ISBN 978-92-9260-334-2
[50] O. B. Fosso, A. Gjelsvik, A. Haugstad, B. Mo, and I. Wangensteen, "Generation scheduling in a deregulated system. the norwegian case," *IEEE Transactions on Power Systems*, vol. 14, no. 1, pp. 75–80, 1999.
[51] J. Zou, S. Ahmed, and X. A. Sun, "Stochastic dual dynamic integer programming," *Mathematical Programming*, pp. 1–42, 3 2018.
[52] K. S. Gjerden, A. Helseth, B. Mo, and G. Warland, "Hydrothermal scheduling in Norway using stochastic dual dynamic programming; a large-scale case study," in *2015 IEEE Eindhoven PowerTech*. IEEE, 6 2015. doi: 10.1109/PTC.2015.7232278. ISBN 978-1-4799-7693-5 pp. 1–6.

Per Aaslid received the M.Sc. degree in engineering cybernetics in 2009 from Norwegian University of Science and Technology (NTNU), Trondheim, Norway. He is a research scientist at SINTEF Energy Research and is currently pursuing the Ph.D. degree with the Department of Electrical Power Engineering (NTNU). His research interests include stochastic optimization, operation of distributed energy storages and hydropower optimization.

Magnus Korpås received his Ph.D. degree from the Norwegian University of Science and Technology (NTNU), Norway, in 2004 on the topic of optimizing the use of energy storage for distributed wind energy in the power market. He is currently working as Professor at the Department of Electric Power Engineering, NTNU, where he also leads the Electricity Markets and Energy System Planning research group. He is a leader and active participant in several large energy research projects at national and European levels. He is a former Research Director of the Department of Energy Systems at SINTEF Energy Research, Norway. He was a visiting researcher in the MIT Laboratory for Information & Decision Systems (LIDS) in 2018-2019. He is also the leader of the scientific committee and the leader of the work package on flexible resources in the power system in the Centre for Intelligent Electricity Distribution (CINELDI).

Michael M Belsnes has a M.Sc. from Technical University of Denmark 1995 and received his PhD degree from NTNU in 2008 on the topic "Optimal Utilization of the Norwegian Hydropower System". In SINTEF Energy Research where he was employed from 1995, he has worked with power system modelling and hydropower scheduling both as researcher and research manager. He is currently managing development and deployment of the scheduling tools deployed by: power producers, the Norwegian regulator, and Nordic TSOs. He is active as sub-program manager in EERA JP HydroPower and JP e3s.

Olav B Fosso is Professor at the Department of Electric Power Engineering of the Norwegian University of Science and Technology (NTNU). He has previously held positions as Scientific Advisor and Senior Research Scientist at SINTEF Energy Research, and Director of NTNUs Strategic Thematic Area Energy from September 2014 - September 2016. He has been Chairman of CIGRE SC C5 Electricity Markets and Regulation and Member of CIGRE Technical Committee (2008 – 2014). He has been expert evaluator in Horizon2020 and in a number of science foundation internationally. His research activities involve hydro scheduling, market integration of intermittent generation and signal analysis for study of power system's dynamics and stability.